Electronic Supplementary Material (ESI) for Lab on a Chip.

Lab on a Chip

Supplementary Information

Tunable Superomniphobic Surfaces for Sorting Droplets by Surface Tension

S. Movafaghi, W. Wang, A. Metzger, D. D. Williams, J. D. Williams and A. K. Kota*

Section 1. Fabrication of devices with discrete solid surface energy domains.

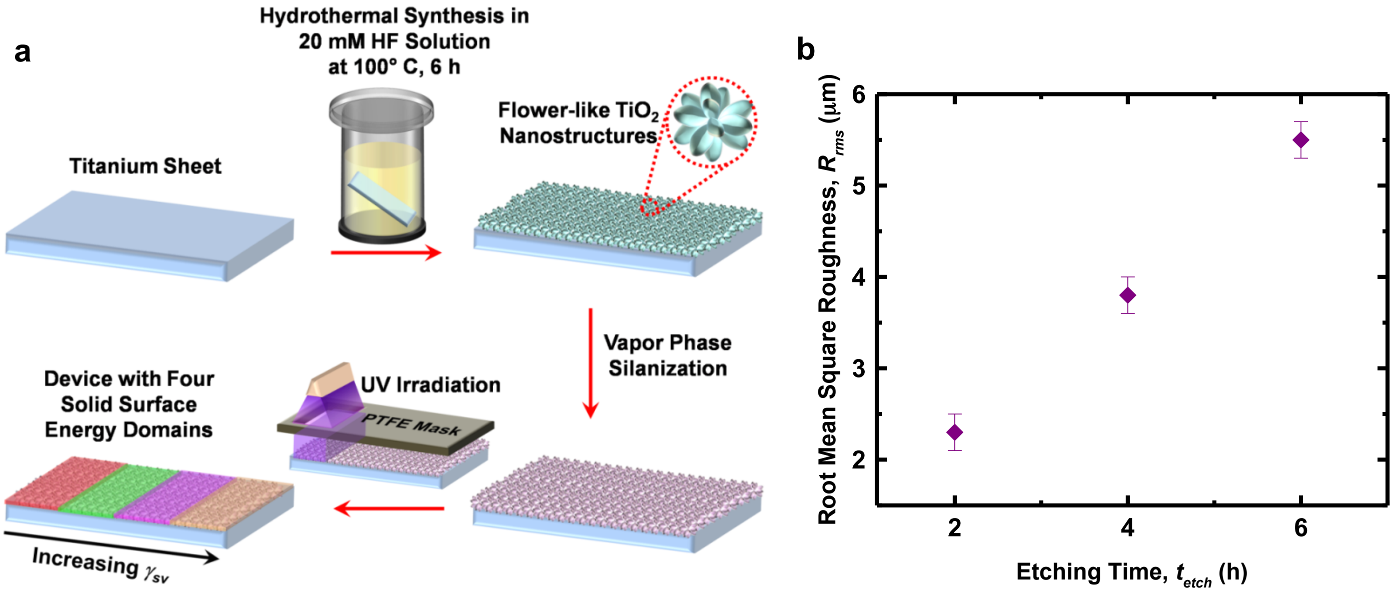

Figure S1. a) Schematic depicting the fabrication of a device with discrete solid surface energy domains. b) The root mean square roughness of the surfaces at different etching times.

Titanium (Ti) sheets (6 cm long × 2 cm wide × 0.8 mm thick) were cleaned by sonication in acetone and isopropanol, dried with nitrogen and placed in a PTFE-lined stainless steel autoclave containing 20 mM hydrofluoric acid (Sigma Aldrich). The autoclave was sealed and the Ti sheets were etched under hydrothermal conditions at 100°C for different times (Figure S1a). As the etching time t_{etch} increased, more TiO_2 nanostructures formed and consequently the roughness R_{rms} of the surface increased (Figure S1b). After hydrothermal synthesis, the samples were rinsed thoroughly with deionized water, dried with nitrogen, and the surface was modified via vapor phase silanization at 120°C for 1 hour using 200 µL of heptadecafluoro-1,1,2,2-tetrahydrodecyl trichlorosilane (Gelest). Superomniphobic surfaces with flower-like TiO_2 nanostructures were obtained by etching under hydrothermal conditions for 6 h or longer. The surface chemistry, and consequently the solid surface energy, of the superomniphobic surfaces with flower-like TiO_2 nanostructures was tuned by UV irradiating the surface for different times using a 254 nm UV bench lamp (UVP XX-40S). The samples were placed approximately 2 cm away from the UV lamp. Devices with discrete solid surface energy domains were fabricated by UV irradiating the desired area of a superomniphobic surface for the desired time while masking the other areas with a PTFE tape. In order to account for droplets of the same liquid (with same surface tension) adhering at slightly different locations (typically < 10 mm from each other) within a discrete domain (due to small variations in droplet volume and surface roughness), we fabricated each discrete domain to be long enough (~15 mm) so that the kinetic energy of the accelerating droplets is completely overcome by the work expended due to adhesion precisely in the first domain where its roll off angle is higher than the tilt angle.

Section 2. Estimation of solid surface energy.

Owens-Wendt[1] approach was used to estimate the solid surface energy γ_{sv} of the fluorinated TiO_2 surfaces before and after UV irradiation. n-hexadecane (γ_{lv} = 27.5 mN m^{-1}) was used as the non-polar liquid to estimate the dispersive component of the solid surface energy γ_{sv}^{d} and water (γ_{lv}^{d}= 21.1 mN m^{-1} and γ_{lv}^{p}= 51.0 mN m^{-1}) was used as the polar liquid to estimate the polar component of the solid surface energy γ_{sv}^{p}. Assuming the advancing contact angle θ_{adv} is approximately equal to Young's contact angle,[2-7] the advancing contact angles measured at different UV irradiation times t_{UV} on fluorinated, non-textured TiO_2 surfaces (see experimental section in the main manuscript) were used to estimate the solid surface energy (Table S1).

Table S1. Advancing contact angles of water and n-hexadecane and solid surface energies, at different UV irradiation times, for fluorinated, non-textured TiO_2 surfaces.

t_{UV} (min)	θ_{adv}		γ_{sv} (mN m^{-1})
	n-hexadecane	Water	
0	80°	120°	10
2	77°	108°	12
4	73°	104°	14
6	69°	97°	17
8	62°	85°	24
10	56°	74°	31

Section 3. Apparent contact angles of different liquids on superomniphobic surfaces before UV irradiation.

The apparent advancing and the apparent receding contact angles of different liquids on superomniphobic surfaces before UV irradiation (t_{UV} = 0 min) are listed in Table S2.

Table S2. The apparent advancing and the apparent receding contact angles of different liquids on superomniphobic surfaces before UV irradiation.

Liquid	Surface tension (mN m^{-1})	θ^*_{adv}	θ^*_{rec}
Water	72.1	164°	162°
Water + 10% Ethanol	53.4	161°	159°
Water + 20% Ethanol	43.7	159°	155°
Water + 30% Ethanol	37.2	156°	153°
Water + 60% Ethanol	28.7	154°	150°
n-hexadecane	27.5	153°	150°

Section 4. Influence of UV irradiation time on solid surface energy, and apparent contact angles and roll off angles of water and n-hexadecane.

The influence of t_{UV} on γ_{sv} and consequently on the apparent advancing and receding contact angles θ^*_{adv} and θ^*_{rec} and roll off angles ω of water and n-hexadecane on our superomniphobic TiO_2 surfaces (i.e., fluorinated surfaces with flower-like TiO_2 nanostructures) is shown in Table S3. It is evident from Table S3 (and Figure 2f of the main manuscript) that θ^*_{adv} and θ^*_{rec} decrease for both n-hexadecane and water with increasing t_{UV}. Further, it is evident that θ^*_{rec} decreases (also see Figure 2f of the main manuscript) and ω increases (also see Figure 2g of the main manuscript) more rapidly for n-hexadecane (lower γ_{lv} liquid) compared to water (higher γ_{lv} liquid) with increasing t_{UV}. In this work, our primary interest lies in $t_{UV} \leq 10$ min because at $t_{UV} \geq 10$ min, n-hexadecane droplets remain adhered and can no longer roll off, i.e., the mobility of n-hexadecane droplets can no longer be tuned or changed. For longer UV irradiation times (i.e., 10 min < t_{UV} < 30 min), our experiments indicate that the apparent receding contact angles of n-hexadecane continue to decrease more rapidly than water. For very long UV irradiation times (i.e., t_{UV} > 30 min), our experiments indicate that the surfaces become superomniphilic (i.e., the apparent contact angles of both water and n-hexadecane are ~0°). It is worth noting that in spite of numerous studies,[8-16] the explicit mechanisms involved in UV-induced wettability of TiO_2 surfaces (including the rate and degree of degradation of organic compounds such as fluorinated groups) are not completely established and continue to be an area of active research.

Table S3. The apparent advancing and receding contact angles and roll off angles of water and n-hexadecane on superomniphobic surfaces after UV irradiation.

t_{UV} (min)	γ_{sv} (mN m^{-1})	θ^*_{adv}		θ^*_{rec}		ω	
		n-hexadecane	Water	n-hexadecane	Water	n-hexadecane	Water
0	10	153°	164°	150°	162°	5°	2°
2	12	144°	162°	125°	155°	16°	3.5°
4	14	139°	158°	114°	151°	27°	5°
6	17	131°	155°	102°	147°	44°	7°
8	24	124°	151°	89°	141°	68°	11°
10	31	120°	144°	70°	134°	No roll off	13°

Section 5. Estimation of roll off angles.

Based on a balance between work done by gravitational force and work expended due to adhesion, the roll off angle ω on a super-repellent surface is given as:[17]

$$\rho g V \sin\omega \approx \gamma_{lv} D_{TCL}\left(\cos\theta^{*}_{rec} - \cos\theta^{*}_{adv}\right) \tag{S1}$$

Here, γ_{lv}, ρ and V are surface tension, density and volume of the liquid droplet, respectively, and g is the gravitational acceleration. θ^{*}_{adv} and θ^{*}_{rec} are the apparent advancing contact angle and the apparent receding contact angle, respectively. D_{TCL} is the width of the triple phase contact line perpendicular to the rolling direction. When the shape of the droplet does not deviate significantly from a spherical cap, the width of the triple phase contact line can be computed as:[18]

$$D_{TCL} = 2\cos\left(\bar{\theta}^{*} - \frac{\pi}{2}\right)\left[\frac{3V}{\pi\left(2 - 3\cos\bar{\theta}^{*} + \cos^{3}\bar{\theta}^{*}\right)}\right]^{\frac{1}{3}} \tag{S2}$$

Here, $\bar{\theta}^{*}$ is the average apparent contact angle, given as:

$$\cos\bar{\theta}^{*} = \frac{\cos\theta^{*}_{adv} + \cos\theta^{*}_{rec}}{2} \tag{S3}$$

The estimated roll off angles of different liquids shown in Figure 2g and Figure 3g of the main manuscript were obtained using Equations S1-S3.

Section 6. Roll off angles of water-ethanol mixtures.

The estimated roll off angles of different water-ethanol mixtures in each of the discrete domains of our device are listed in Table S4 (also see Figure 3g of the main manuscript).

Table S4. Apparent advancing and apparent receding contact angles, and the estimated roll off angles of different water-ethanol mixtures in each of the discrete domains shown in Figures 3b-3f of the main manuscript.

		Water	Water +10% Ethanol	Water +20% Ethanol	Water +30% Ethanol	Water +60% Ethanol
Surface tension (mN m^{-1})		72.1	53.4	43.7	37.2	28.7
Domain 1	θ^*_{adv}	162°	158°	156°	150°	145°
(t_{UV} = 2 min;	θ^*_{rec}	155°	150°	147°	141°	121°
γ_{sv} = 12 mN m^{-1})	ω	3°	3°	4°	5°	17°
Domain 2	θ^*_{adv}	158°	152°	146°	141°	140°
(t_{UV} = 4 min;	θ^*_{rec}	151°	140°	132°	117°	111°
γ_{sv} = 14 mN m^{-1})	ω	4°	8°	11°	24°	27°
Domain 3	θ^*_{adv}	155°	143°	140°	132°	131°
(t_{UV} = 6 min;	θ^*_{rec}	147°	132°	109°	101°	95°
γ_{sv} = 17 mN m^{-1})	ω	6°	11°	44°	46°	47°
Domain 4	θ^*_{adv}	151°	129°	127°	126°	122°
(t_{UV} = 8 min;	θ^*_{rec}	141°	115°	95°	90°	81°
γ_{sv} = 24 mN m^{-1})	ω	9°	24°	74°	82°	84°

It is evident from Table S4 that all of our UV irradiated surfaces used to fabricate the device have finite roll off angles ($\omega < 90°$) with the liquids listed. While these liquid droplets may adhere to a UV irradiated surface at low tilt angles ($\alpha < \omega$), they roll off from the UV irradiated surface at higher tilt angles ($\alpha > \omega$). If the droplets were completely in the Wenzel state, they would remain adhered to the surface and no longer exhibit mobility (i.e., droplets would not have a finite roll off angle ω). Based on this, we conclude that the droplets on the UV irradiated surfaces used to fabricate the device (e.g., Figures 3b-3f of the main manuscript) are primarily in the Cassie-Baxter state.

Further, it is evident from Table S4 that the contact angle hysteresis of droplets with lower surface tension is higher than that of droplets with higher surface tension. Contact angle hysteresis primarily arises from surface roughness and heterogeneity.[19-21] It is related to the energy barriers that a liquid droplet must overcome during its movement along a solid surface, and thus characterizes the resistance to droplet movement.[19-21] Typically, the resistance to droplet movement is higher for lower surface tension liquids compared to higher surface tension liquids.[22] This is possibly because lower surface tension liquids have higher solid-liquid contact area (and longer triple phase contact line), which in turn is due to their lower contact angles. Consequently, on our tunable superomniphobic surfaces, for any given solid surface energy, the contact angle hysteresis of droplets with lower surface tension is higher than that of droplets with higher surface tension.

Section 7. Reusability of our devices.

In order to evaluate the reusability of our devices, we first wet each discrete solid surface energy domain with an extremely low surface tension liquid (e.g., ethanol; γ_{lv} = 22.1 mN m^{-1}) that remained adhered to the surface. Then, we completely dried the liquid on the surface by heating. Subsequently, we measured the roll off angles of different liquids in each domain to verify that the surface repellence has not been altered. Our experiments indicated that the roll off angles of different liquids in each domain remained unaltered even after a few wetting/drying cycles. To illustrate this with an example, here we present (Figure S2) the measured roll off angles of different liquids (water, water + 10% ethanol, water + 20% ethanol, water + 30% ethanol, and water + 60% ethanol) on one of the domains with γ_{sv} = 12 mN m^{-1} after wetting with ethanol and subsequently drying for 25 times. The functionality of the device remains un-altered up to 25 cycles. As we increase the number of cycles further, the range over which we can sort droplets by surface tension decreases. This is because the re-entrant texture of our superomniphobic surfaces starts to deteriorate with increased cycles. This in turn causes the low surface tension liquid droplets to adopt the Wenzel state (and consequently, the droplet mobility can no longer be tuned) at increasingly more locations on the surface. Here, it is worth noting that improving the mechanical durability of superomniphobic surfaces continues to be a grand challenge in the field of surface science.

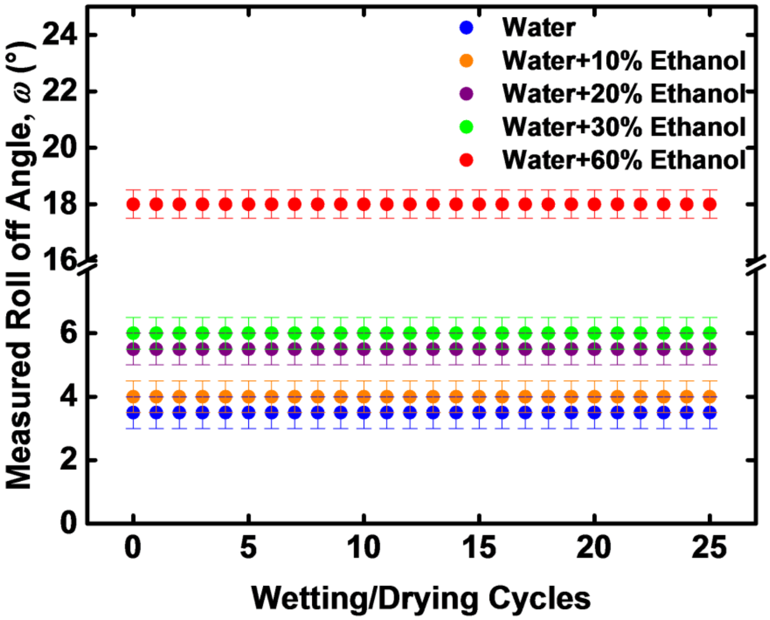

Figure S2. The measured roll off angles of different liquids on the domain with γ_{sv} = 12 mN m^{-1} after wetting with ethanol and subsequently drying, for 25 times.

References:

1. D. Owen and R. Wendt, *J. Appl. Polym. Sci.*, 1969, **13**, 1741.
2. A. Neumann, *Adv. Colloid Interface Sci.,* 1974, **4**, 105.
3. D. Y. Kwok and A. W. Neumann, *Adv. Colloid Interface Sci.*, 1999, **81**, 167.
4. A. Tuteja, W. Choi, M. Ma, J. M. Mabry, S. A. Mazzella, G. C. Rutledge, G. H. McKinley and R. E. Cohen, *Science*, 2007, **318**, 1618.
5. A. Tuteja, W. Choi, J. M. Mabry, G. H. McKinley and R. E. Cohen, *Proc. Natl. Acad. Sci. U.S.A.*, 2008, **105**, 18200.
6. A. K. Kota, G. Kwon, W. Choi, J. M. Mabry and A. Tuteja, *Nat. Commun.*, 2012, **3**, 1025.
7. A. K. Kota, Y. Li, J. M. Mabry and A. Tuteja, *Adv. Mater.*, 2012, **24**, 5838.
8. R. Wang, K. Hashimoto, A. Fujishima, M. Chikuni, E. Kojima, A. Kitamura, M. Shimohigoshi and T. Watanabe, *Nature*, 1997, **388**, 431.
9. R. Wang, K. Hashimoto, A. Fujishima, M. Chikuni, E. Kojima, A. Kitamura, M. Shimohigoshi and T. Watanabe, *Adv. Mater.*, 1998, **10**, 135.
10. R. Wang, N. Sakai, A. Fujishima, T. Watanabe and K. Hashimoto, *J. Phys. Chem. B*, 1999, **103**, 2188.
11. T. Watanabe, A. Nakajima, R. Wang, M. Minabe, S. Koizumi, A. Fujishima and K. Hashimoto, *Thin solid films*, 1999, **351**, 260.
12. N. Sakai, A. Fujishima, T. Watanabe and K. Hashimoto, *J. Phys. Chem. B*, 2003, **107**, 1028.
13. C.-y. Wang, H. Groenzin and M. J. Shultz, *Langmuir*, 2003, **19**, 7330.
14. J. M. White, J. Szanyi and M. A. Henderson, *J. Phys. Chem. B*, 2003, **107**, 9029.
15. M. Takeuchi, K. Sakamoto, G. Martra, S. Coluccia and M. Anpo, *J. Phys. Chem. B*, 2005, **109**, 15422.
16. T. Zubkov, D. Stahl, T. L. Thompson, D. Panayotov, O. Diwald and J. T. Yates, *J. Phys. Chem. B*, 2005, **109**, 15454.
17. C. G. L. Furmidge, *J. Coll. Sci.*, 1962, **17**, 309.
18. W. Choi, A. Tuteja, J. M. Mabry, R. E. Cohen and G. H. McKinley, *J. Colloid Interface Sci.*, 2009, **339**, 208.
19. R. Dettre and R. Johnson, *Adv. Chem. Ser.*, 1964, **43**, 112.
20. R. H. Dettre and R. E. Johnson Jr, *J. Phys. Chem.*, 1965, **69**, 1507.
21. R. E. Johnson Jr and R. H. Dettre, *J. Phys. Chem.*, 1964, **68**, 1744.
22. E. Bormashenko, R. Pogreb, G. Whyman, Y. Bormashenko and M. Erlich, *Appl. Phys. Lett.*, 2007, **90**, 201917.

Movie Legends

Movie S1. This video illustrates a droplet of water + 60% ethanol bouncing on the superomniphobic TiO_2 surface tilted by 2° relative to the horizontal. The droplet was released from 4 mm above the surface. High speed movies were obtained using a high speed camera (Photron FASTCAM SA3) at 2000 frames per second.

Movie S2. This video illustrates that before UV irradiation a superomniphobic surface tilted by 15° relative to the horizontal allows both water and n-hexadecane droplets to freely roll past the surface. However, after UV irradiation for 6 minutes, the surface tilted by 15° relative to the horizontal allows water droplets to roll off, but n-hexadecane droplets are trapped by (or remain adhered to) the surface.

Movie S3. This video illustrates sorting of ~5 μL liquid droplets with different surface tension values using a device with four discrete surface energy domains tilted at an angle of 15° relative to the horizontal. Each domain allows certain high surface tension liquid droplets to freely roll past the surface while trapping other low surface tension liquid droplets due to adhesion.